IOPscience iopscience.iop.org

Home Search Collections Journals About Contact us My IOPscience

Magnetic properties and atomic configurations of the ternary alloys Ru - Mn - Z (Z = Si, Ge and Sn)

This article has been downloaded from IOPscience. Please scroll down to see the full text article.

1996 J. Phys.: Condens. Matter 8 6889

(http://iopscience.iop.org/0953-8984/8/37/010)

View the table of contents for this issue, or go to the journal homepage for more

Download details:
IP Address: 171.66.16.206
The article was downloaded on 13/05/2010 at 18:40

Please note that terms and conditions apply.

J. Phys.: Condens. Matter **8** (1996) 6889–6899. Printed in the UK

Magnetic properties and atomic configurations of the ternary alloys Ru–Mn–Z (Z = Si, Ge and Sn)

S Ishida†, S Kashiwagi†, S Fujii† and S Asano‡

† Department of Physics, Faculty of Science, Kagoshima University, Kagoshima, 890, Japan
‡ Institute of Physics, College of Arts and Sciences, University of Tokyo, Meguro-ku, Tokyo, 153, Japan

Received 12 April 1996, in final form 4 June 1996

Abstract. The electronic structures of the ternary alloys Ru–Mn–Z (Z = Si, Ge and Sn) were calculated to examine the relationship between the magnetic properties and the atomic configurations. It will be shown that two types of antiferromagnetic phase are stable for three types of configuration of those alloys, where the Mn magnetic moments are aligned ferromagnetically in the (100) (or (111)) plane and antiparallel along the [100] (or [111]) direction. It will also be shown that Ru–Mn–Z (Z = Si and Ge) can be half-metallic in a ferromagnetic phase.

1. Introduction

Most of the Heusler alloys with the $L2_1$ crystal structure are ferromagnets if they are magnetic at all. Recently, new Heusler alloys Ru_2MnZ (Z = Si, Ge, Sn and Sb) were prepared by Kanomata *et al* (1993), and Gotoh *et al* (1995) showed from the neutron diffraction patterns that Ru_2MnGe and Ru_2MnSb exhibit antiferromagnetic ordering. The Mn atoms are the only carriers of the magnetic moment in the antiferromagnetic ordering and the moments align along the [111] axis. The electronic structures of these alloys were calculated and it was theoretically predicted that the observed antiferromagnetic order is stable (Ishida *et al* 1995).

Kanomata (1995) also prepared the ternary alloys Ru–Mn–Z (Z = Si, Ge and Sn) and the crystal structure was determined to be the $C1_b$-type crystal structure. This structure is closely related to the $L2_1$ structure; one site of two Ru sites of Ru_2MnZ is vacant in the structure of RuMnZ. Gotoh (1995) also showed from a neutron diffraction experiment on Ru–Mn–Si that the observed magnetic order is the same as that of Ru_2MnGe and Ru_2MnSb—that is, antiferromagnetic order. However, atomic disorder was observed in the sample used, where fifty per cent of the Mn atoms were replaced by Ru atoms. The temperature dependence of the magnetic susceptibility was also measured and it was found that the values below the Néel temperature were sensitive to the heat treatment conditions. We guess from the features that some atomic configurations mix in the sample.

In this situation, it is interesting to examine how the atomic configurations affect the magnetic properties of Ru–Mn–Z (Z = Si, Ge and Sn). Three atomic configurations are possible for the $C1_b$ structures. We calculated the electronic structures of Ru–Mn–Z (Z = Si, Ge and Sn) for these configurations and will discuss the relationship between the magnetic properties and the atomic configurations on the basis of the electronic structures obtained.

0953-8984/96/376889+11$19.50 © 1996 IOP Publishing Ltd

Table 1. The atomic sites for the four magnetic phases in the XYZ-type configuration.

Phase	Name	Atom	Atomic site	
f	4a	Y	(0, 0, 0)	
g216	4b	Z	(1/2, 1/2, 1/2)	
$F\bar{4}3m$	4c	X	(1/4, 1/4, 1/4)	
$C1_b$	4d	Empty	(3/4, 3/4, 3/4)	
af 1	2a	Y(1)	(0, 0, 0), (1/2, 1/2, 0)	
g113	2c	Y(2)	$(0, 1/2, z), (1/2, 0, -z)$	$z = 1/2$
$P\bar{4}2_1m$	2b	Z(1)	(0, 0, 1/2), (1/2, 1/2, 1/2)	
	2c	Z(2)	$(0, 1/2, z), (1/2, 0, -z)$	$z = 0$
	4e	X	$(x, x + 1/2, -z), (-x, -x + 1/2, z)$ $(x + 1/2, -x, -z), (-x + 1/2, x, -z)$	$x = 1/4, z = 3/4$
	4e	Empty	$(x, x + 1/2, -z), (-x, -x + 1/2, z)$ $(x + 1/2, -x, -z), (-x + 1/2, x, -z)$	$x = 3/4, z = 1/4$
af 2			(0, 0, 0)+, (2/3, 1/3, 1/3)+, (1/3, 2/3, 2/3)+	
g160	3a	Y(1)	$(0, 0, z)$	$z = 0$
$R3m$	3a	Y(2)	$(0, 0, z)$	$z = 1/2$
	9b	Z(1)	$(x, -x, z), (x, 2x, z), (-2x, -x, z)$	$x = 2/3, z = 1/12$
	9b	Z(2)	$(x, -x, z), (x, 2x, z), (-2x, -x, z)$	$x = 1/3, z = 11/12$
	9b	X(1)	$(x, -x, z), (x, 2x, z), (-2x, -x, z)$	$x = 2/3, z = 23/24$
	3a	X(2)	$(0, 0, z)$	$z = 1/8$
	9b	Empty(1)	$(x, -x, z), (x, 2x, z), (-2x, -x, z)$	$x = 1/3, z = 1/24$
	3a	Empty(2)	$(0, 0, z)$	$z = 7/8$
af 3	4a	Y(1)	(0, 0, 0), (1/2, 0, 3/4)	
g122	4b	Y(2)	(0, 0, 1/2), (1/2, 0, 1/4)	
$I\bar{4}2d$	8c	Z	$(0, 0, z), (0, 0, -z), (1/2, 0, -z + 3/4)$ $(1/2, 0, z + 3/4)$	$z = 1/4$
	8d	X	$(x, 1/4, 1/8), (-x, 3/4, 1/8)$ $(1/4, -x, 7/8), (3/4, x, 7/8)$	$x = 1/4$
	8d	Empty	$(x, 1/4, 1/8), (-x, 3/4, 1/8)$ $(1/4, -x, 7/8), (3/4, x, 7/8)$	$x = 3/4$

2. Crystal structure and the method of calculation

The crystal structure of Ru–Mn–Z alloys is of the $C1_b$ type, where one atomic site is vacant in two Ru atomic sites of the $L2_1$-type Ru_2MnZ. In this calculation, an empty lattice is placed on the vacant site. As described already, fifty per cent of the Mn atoms are replaced by Ru atoms in the sample used for the experiment. Thus, there is the possibility that the magnetic Mn atoms are in some different circumstances and affect the magnetic properties of Ru–Mn–Z. Here, three types of atomic configuration (XYZ, YXZ and ZYX types) are considered; these are shown in figure 1. The Mn atoms are surrounded by four nearest Ru atoms in RuMnZ (XYZ type), by four Ru and four Z atoms in MnRuZ (YXZ type) and by four Z atoms in ZMnRu (ZYX type). In the following description, we distinguish the chemical formulas of RuMnZ, MnRuZ and ZMnRu that represent the ternary alloys in the different atomic configurations. When we do not distinguish the configuration, the alloy is described as 'Ru–Mn–Z'. We also consider four magnetic phases to examine a stable magnetic phase—that is, a ferromagnetic (f) and three antiferromagnetic phases (af 1, af 2 and af 3). The configurations of Mn magnetic moments in these magnetic phases are shown in figure 2. The af 1 and af 2 phases are characterized by alternating ferromagnetic planes

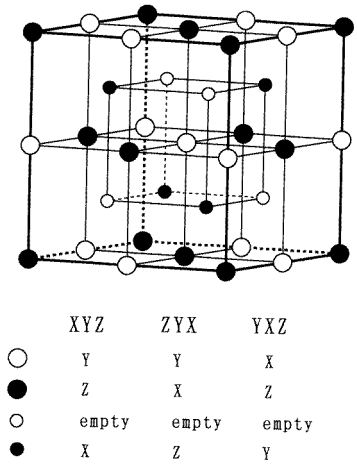

Figure 1. The crystal structure of the ternary alloy X–Y–Z of $C1_b$ type for three types of atomic configuration.

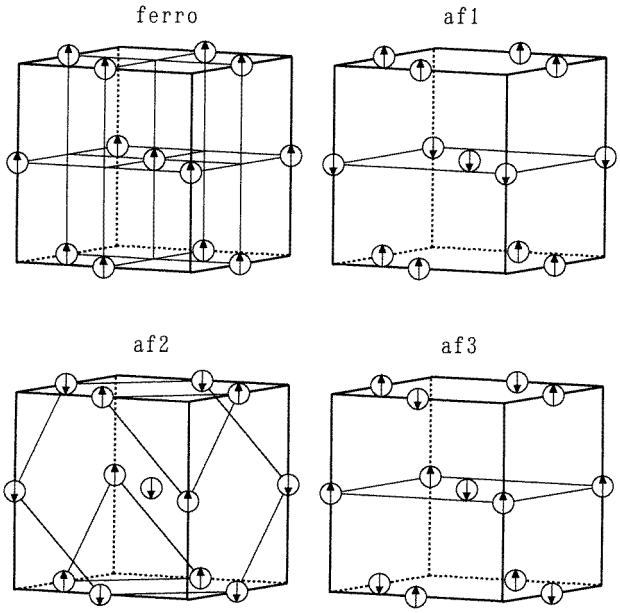

Figure 2. The configuration of the Mn magnetic moment in Ru–Mn–Z. The ferromagnetic configuration is indicated by ferro and the three types of antiferromagnetic configuration by af 1, af 2 and af 3.

of up and down moments perpendicular to the [100] and [111] directions, respectively. In the af 3 phases, adjacent moments along two of the cube edges are aligned parallel and along the other are aligned antiparallel. The numbers of space groups for the f, af 1, af 2 and af 3 phases are assumed to be 216, 113, 160 and 122 in the *International Tables for Crystallography* (Hahn 1983). The atomic sites and the positional parameters are listed in table 1 for the XYZ configuration, where X and Y atoms correspond to Ru and Mn atoms and the empty lattice is indicated as 'empty'. In the antiferromagnetic phases, the Mn atoms with up and down moments are distinguished by Y(1) and Y(2). The X and Z atoms and the

empty lattice are also distinguished as X(1), X(2) etc when their circumstances are different because of the directions of the Mn moments.

The energy eigenvalues were determined by the LMTO-ASA method in the non-relativistic approximation (Andersen 1975, Andersen and Jepsen 1984, Andersen *et al* 1985, Skriver 1984) and the exchange–correlation potentials were treated within the framework of the LSD approximation (Janak *et al* 1975). The combined correction term was neglected and the energies and eigenvectors are correct to third order of $E - E_\nu$ which is the difference between the exact and fixed energies. Considering that the volumes of the primitive cells for the af 1, af 2 and af 3 phases are 4, 2 and 4 times larger than that for the f phase, we chose 2048, 512, 1385 and 512 $\boldsymbol{k}$ mesh points in the Brillouin zones for the f, af 1, af 2 and af 3 phases, respectively. We prepared several sets of the radii of the atomic spheres to find reasonable equilibrium lattice parameters and the following was finally used: the ratio of the radii is R_{Ru}:R_{Mn}:R_Z:R_{emp} = 1.05:1.0:1.06:0.95 for Z = Si, =1.06:1.0:1.09:0.95 for Z = Ge, and =1.29:1.0:1.06:0.95 for Z = Sn. The radii used here produce reasonable results for the lattice constant as seen later. The maximum angular momenta to describe the valence states were chosen to be $l_{max} = 2$ for all of the atoms. The density of states was determined by the tetrahedral integration method (Lehmann *et al* 1970, Lehmann and Taut 1972, Jepsen and Andersen 1971, Rath and Freeman 1975).

Table 2. The lattice constant and the Mn magnetic moment of the ternary alloy Ru–Mn–Z for the four magnetic phases in the three atomic configurations.

Ru–Mn–Z	Magnetic phase	Lattice constant (Å)			Moment on Mn (μ_B)		
		Z = Si	Z = Ge	Z = Sn	Z = Si	Z = Ge	Z = Sn
XYZ type	f	5.77	5.87	6.27	1.38	1.57	4.00
	af 1	5.82	5.93	6.25	2.56	3.02	3.86
	af 2	5.84	5.95	6.26	2.75	3.20	3.93
	af 3	5.81	5.93	6.25	2.40	2.96	3.85
ZYX type	f	5.85	5.95	6.10	3.53	3.69	3.72
	af 1	5.84	5.95	6.10	3.41	3.72	3.73
	af 2	5.85	5.94	6.10	3.51	3.70	3.74
	af 3	5.84	5.95	6.10	3.42	3.70	3.74
YXZ type	f	5.80	5.90	6.29	0.19	0.37	2.78
	af 1	5.84	5.94	6.27	1.67	2.08	2.73
	af 2	5.82	5.94	6.29	1.20	1.98	2.79
	af 3	5.83	5.99	6.28	1.45	2.25	2.77
Experiment	af 2	5.851	5.978	6.219			

3. Total energy and the ground magnetic phase

The total energies for Ru–Mn–Z (Z = Si, Ge and Sn) were calculated as functions of the lattice constant a and are shown in figure 3. The four marked curves distinguish the f, af 1, af 2 and af 3 phases in the three types of atomic configuration. It is found from the figures that the stable configuration is of the XYZ type for the cases where Z = Si and Z = Ge and of the ZYX type for the case where Z = Sn, and the stable magnetic phase is the af 1 phase for the XYZ and YXZ types and the af 2 phase for the ZYX type. The af 2 phase

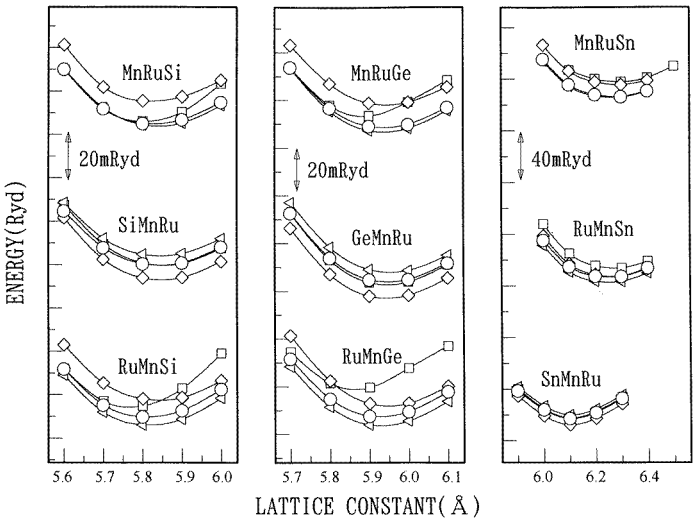

Figure 3. The lattice constant dependence of the total energy per formula unit for Ru–Mn–Si, Ru–Mn–Ge and Ru–Mn–Sn. Squares, triangles, diamonds and circles correspond to the f, af 1, af 2 and af 3 phases.

was observed for Z = Si but the sample is not in a single-phase structure (Gotoh 1995). The theoretical values of the lattice constant were determined so as to minimize the total energies. The values are listed in table 2 and are compared with the experimental values. The theoretical value is slightly smaller than the observed values for the f phase but their agreement is reasonable for the af 1, af 2 and af 3 phases. In the next section, we will look at the density of states (DOS) for the theoretical lattice constants.

4. The ferromagnetic phase of Ru–Mn–Sn

We first investigate the (DOS) of a ferromagnetic phase of Ru–Mn–Sn and examine the effect of the atomic configuration on the magnetic properties. Since the Mn atom is the main carrier of the magnetic moment of the alloys, the local DOSs are shown only for Mn d states in figure 4, where from the top to the bottom the panels are for RuMnSn, MnRuSn and SnMnRu. The DOS curves of up (majority) spins and down (minority) spins are drawn as full and dashed lines, respectively, and the Fermi level as a vertical line.

Since the Mn atom in SnMnRu is surrounded by four nearest Sn atoms, the interaction between Mn and Ru atoms is considered to be the smallest among the three atomic configurations. As seen at the bottom of figure 4, the local DOS of Mn d states shows that the d bands of the two spin states are widely separated and this separation produces a large magnetic moment at Mn sites (3.7 μ_B). Although the separation between the DOSs of the two spin states is also seen for Ru and Sn (not shown here), their magnetic moments are negligibly small because the numbers of occupied states are nearly equal for the two spin states. The valence states of the Mn, Ru and Sn atoms have peaks in the DOS at the same energy values. This suggests that the valence states hybridize with each other.

Since the Mn atom in RuMnSn is surrounded by four nearest Ru atoms, the hybridization between the d states of Mn and Ru becomes stronger as compared with that in SnMnRu and the hybridizing energy ranges are different. Therefore, the DOSs of RuMnSn are different

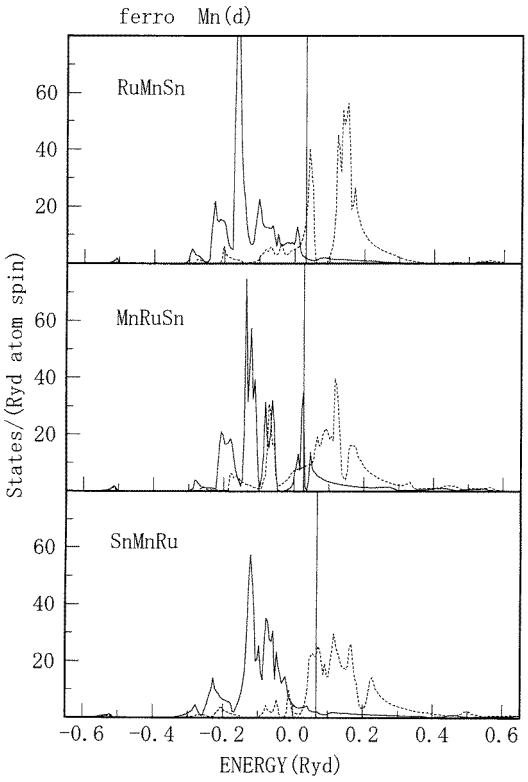

Figure 4. The local DOS curves of the Mn d states in RuMnSn, MnRuSn and SnMnRu for a ferromagnetic phase. The full and dotted curves show the DOSs of up-spin and down-spin states, respectively. The Fermi level is shown by vertical lines.

from those of SnMnRu. It is characteristic that there is a peak just above the Fermi level in the DOS of the down-spin state. Since the peaks are unoccupied, the moment on the Mn atom is larger (4.0 μ_B) in RuMnSn than in SnMnRu.

In MnRuSn, the Mn atom is surrounded by four Ru and four Sn atoms. Therefore, the interaction between the valence states of the Mn atom and the neighbour atoms is the strongest among those of SnMnRu, RuMnSn and MnRuSn. The characteristic of the DOS of MnRuSn is that there is a peak near -0.075 Ryd in the DOS of the down-spin state of Mn. The valence states of Mn, Ru and Sn hybridize well in this energy range. Since the peaks of the down-spin state are below the Fermi level, the magnetic moment on the Mn atom is the smallest (2.78 μ_B) among those of the three atomic configurations.

As described above, the Mn d bands are sensitive to the surroundings, and the magnitudes of the magnetic moment are fairly different in the different atomic configurations of Ru–Mn–Sn.

5. The antiferromagnetic phase of Ru–Mn–Sn

We next look at the DOSs of three antiferromagnetic phases of Ru–Mn–Sn. Those of RuMnSn for the af 1, af 2 and af 3 phases are compared in figure 5. Comparing the DOS

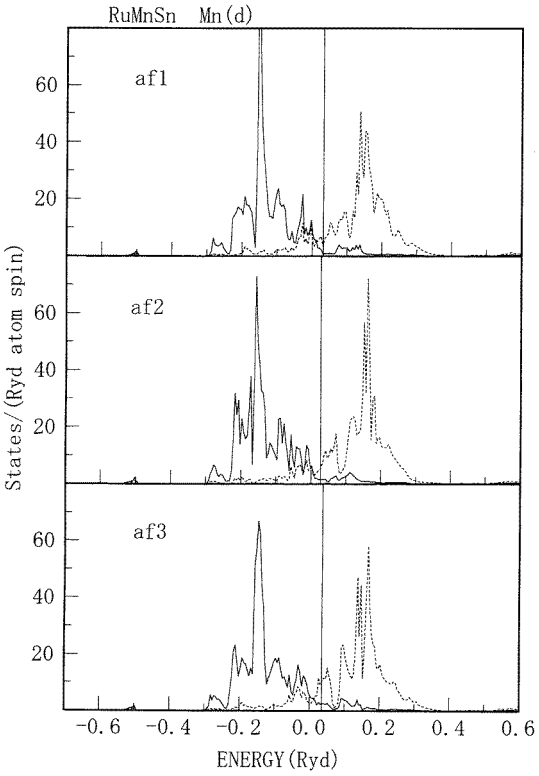

Figure 5. The local DOS curves of the Mn d states of RuMnSn for af 1, af 2 and af 3 phases.

shapes of the f and af 1 phases of RuMnSn, we find that the sharp peak of the down-spin state just above the Fermi level in the f phase (at the top of figure 4) is not seen in the af 1 phase (at the top of figure 5). The sharp peak in the f phase comes from the hybridization between the d states of the Mn and Ru atoms. In the af 1 phase, the Ru atoms are nonmagnetic due to the symmetry, and the DOSs of the Ru atom are not separated but are equivalent for the two spin states. Therefore, the d states of the Mn and Ru atoms hybridize in different energy ranges for the f and the af 1 phase. As a result, the sharp peak of the down-spin state becomes a low hump and the energy gap near 0.075 Ryd disappears in the af 1 phase. In the af 3 phase, the Ru and Sn atoms are also nonmagnetic because of the symmetry. In the af 2 phase, the Mn atom is surrounded by two types of Ru atom that have antiparallel magnetic moments (the magnitudes are smaller than 0.05 μ_B). Thus, the valence states of the neighbours of the Mn atom are different for different magnetic phases and affect the DOS of the Mn atoms. The antiferromagnetic DOS curves of Mn are fairly different in detail from the ferromagnetic ones but the general features are similar for the af 1, af 2 and af 3 phases.

Although the DOSs are not shown here for SnMnRu and MnRuSn, their characteristics are as follows. As described for the case of the f phase, since the Mn atom in SnMnRu is surrounded by four nearest Sn atoms, the influence of the neighbours is the smallest among those of the three atomic configurations. Therefore, the DOS shapes of the af 1, af 2 and af 3 phases are not so different from those of the f phase. The values of the Mn magnetic

moments in those antiferromagnetic phases are nearly equal to that (3.72 μ_B) in the f phase as seen in table 2.

In MnRuSn, the Mn atoms are mostly affected by the neighbours among the three atomic configurations. As compared with the ferromagnetic DOS, a sharp peak near the Fermi level disappears in the DOS of the up-spin state. However, the characteristic peak near -0.075 Ryd is also seen in the DOS of the down-spin state for the antiferromagnetic phases. The Mn magnetic moments are nearly the same for the four magnetic phases as seen in table 2.

6. Comparison between the electronic structures of Ru–Mn–Z (Z = Si, Ge, Sn)

In the previous sections, we looked the characteristics of the DOSs in the different atomic configurations and the different magnetic phases for the alloy Ru–Mn–Sn. In the following, we study the changes in the DOSs and magnetic properties due to replacing Sn by Si or Ge.

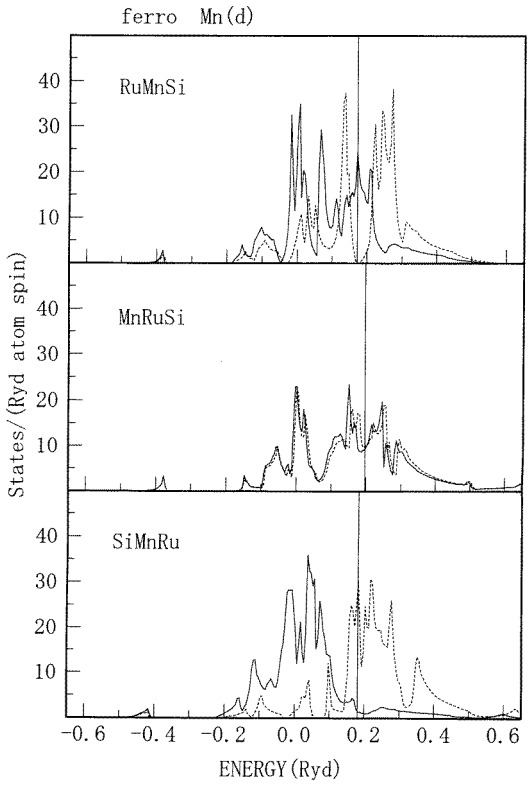

Figure 6. The local DOS curves of the Mn d states in Ru–Mn–Si for three atomic configurations of XYZ, ZYX and YXZ types.

We listed the theoretical and experimental values of the lattice constants in table 2. Comparing these values, we notice that the lattice constant and the Mn magnetic moment become larger in the order of Z = Si, Ge and Sn for all of the configurations of XYZ, ZYX and YXZ types. To examine the cause of this, we compare the ferromagnetic DOSs for

the case of Z = Si with those for Z = Sn in figure 4. The DOSs for the case of Z = Si are shown in figure 6 for the three configurations. For the case of the large lattice constant (Z = Sn), the DOSs of the two spin states are widely separated. As the lattice constant becomes small (Z = Si), the d electrons of Mn become more itinerant, the d bands widen and the overlap between the two spin bands increases. This tendency is strong for the YXZ type where the effect of the neighbours is strong (the middle of figures 4 and 6) and weak for the ZYX type where the effect of the neighbours is weak (the bottom of figures 4 and 6). In the XYZ and YXZ types, the difference of the lattice constants between the cases where Z = Sn and Z = Ge is two times larger than that between the cases where Z = Ge and Z = Si. Therefore, the changes in the DOSs and the magnetic moments are larger for the former replacement than for the latter replacement and the DOSs of Ru–Mn–Ge are similar to those of Ru–Mn–Si.

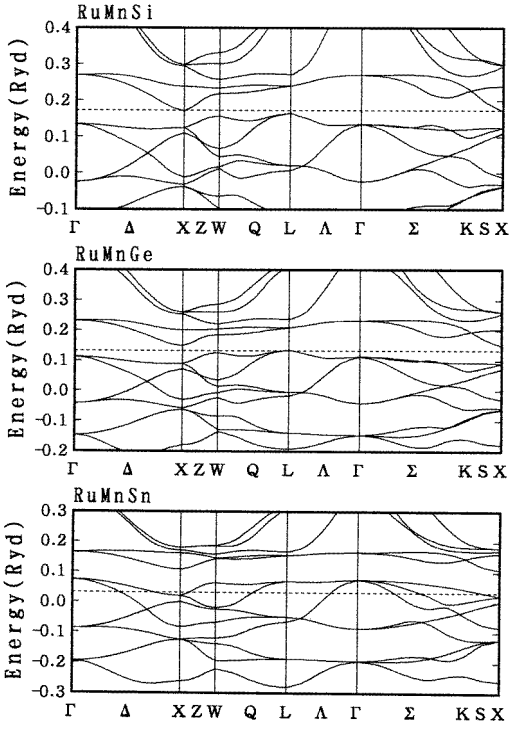

Figure 7. The energy dispersion curves of the down-spin state for RuMnSi, RuMnGe and RuMnSn for the theoretical lattice constant. The Fermi level is shown by a horizontal line in each panel.

The values of the magnetic moments on the Mn atoms are also listed in table 2 for the antiferromagnetic phases. The moments in each configuration of Ru–Mn–Sn are nearly equal for the four magnetic phases. This is also true for the cases where Z = Si and Z = Ge in the ZYX type where the Mn atom has no nearest Ru atom. On the other hand, the moments in the different magnetic phases are different for the cases where Z = Si and Z = Ge in the XYZ and YXZ types where the Mn atom has nearest Ru atoms. These features suggest that the hybridization between the d states of Mn and Ru atoms becomes so strong that it affects the magnetic moment for lattice constants smaller than $a = 6.2$ Å.

7. Half-metallic alloys

We reported that among the alloys Ru_2MnZ (Z = Si, Ge, Sn and Sb), the alloys with Z = Si and Z = Sb can be half-metallic in the f phase, though they are not so in the stable af 2 phase (Ishida *et al* 1995). That is, in a ferromagnetic phase, Ru_2MnZ (Z = Si and Sb) shows normal metallic behaviour for the up-spin state while at the same time being a semiconductor for the down-spin state. We also examine for the $C1_b$-type alloys whether they can be half-metallic or not.

To clarify this, we examined the energy dispersion curves ($E(\boldsymbol{k})$-curves) near the Fermi level at the theoretical lattice constant. It was found that an energy gap is not found in the YXZ type and two energy gaps are found at around 0.1 Ryd and 0.2 Ryd below the Fermi level in the ZYX type but the alloys of this type are not half-metallic. On the other hand, there is a possibility that they are half-metallic for the XYZ type among the three atomic configurations. The $E(\boldsymbol{k})$-curves in the XYZ configuration are shown in figure 7 for the down-spin state of RuMnZ (Z = Si, Ge and Sn). The Fermi level shown by a horizontal dotted line touches the bottom of the conduction band for RuMnSi and the top of the valence band for RuMnGe. The energy curves cross the Fermi level for RuMnSn. There is no energy gap in the energy bands of the up-spin state as seen in figure 4. These facts suggest that RuMnSi and RuMnGe may be half-metallic owing to the changing circumstances. When we changed the lattice constant from the theoretical value to $a = 5.8$ Å, the Fermi level moved in the energy gap and they were confirmed as being half-metallic. Thus, our results suggest that RuMnZ (Z = Si and Sb) in the f phase can be half-metallic near $a = 5.8$ Å, which is slightly smaller as compared with the experimental value ($a = 5.851$ Å for RuMnSi, $a = 5.978$ Å for RuMnGe).

8. Summary

The electronic structures of the ternary alloys Ru–Mn–Z (Z = Si, Ge and Sn) were calculated to examine the relationship between the magnetic properties and the atomic configurations. The alloys have the $C1_b$ crystal structure where three types of atomic configuration are possible. According to our results, the most stable atomic configuration is of the XYZ type for the cases where Z = Si and Z = Ge and of the ZYX type for the case where Z = Sn, and the most stable magnetic phase is the af 1 phase for the XYZ and YXZ types and the af 2 phase for the ZYX type. The magnitude of the magnetic moment on the Ru atom is negligibly small but the moments on the Mn atoms are large and depend on the atomic configuration and the magnetic phase as shown in table 2. These features come from the difference in hybridization between the Mn d states and the valence states of the neighbours and are clearly reflected in the Mn DOS. For RuMnSi, the af 2 phase was observed by a neutron diffraction experiment but at the same time the atomic disorder was confirmed in the sample used. The observed magnetic susceptibility strongly depends on the conditions of the sample preparation. Considering these facts, we guess that the atomic configurations considered in this paper may mix in the samples used for the experiments and the different magnetic states were observed for the different samples. We expect that further experiments will be carried out for the single-phase samples and our results will be useful for the analysis of the experimental results.

It was also found that RuMnZ (Z = Si and Ge) in the ferromagnetic phase can be half-metallic for lattice constants slightly smaller than the experimental value.

Acknowledgments

We would like to thank Professor Y Yamaguchi at Tohoku University and Professor T Kanomata at Tohoku-Gakuin University for providing us with valuable information. This work was partially supported by a Grant-in-Aid for Scientific Research from the Ministry of Education, Science, Culture and Sports of Japan.

References

Andersen O K 1975 *Phys. Rev.* B **12** 3060
Andersen O K and Jepsen O 1984 *Phys. Rev. Lett.* **53** 2571
Andersen O K, Jepsen O and Glotzel D 1985 *Highlights of Condensed-Matter Theory* ed F Bassani *et al* (New York: North-Holland) p 59
Gotoh M 1995 *Thesis* Institute for Materials Research, Tohoku University
Gotoh M, Ohashi M, Kanomata T and Yamaguchi Y 1995 *Physica* B **213–214** 306
Hahn T 1983 (ed) *International Tables for Crystallography* vol A (Boston, MA: Reidel)
Ishida S, Kashiwagi S, Fujii S and Asano S 1995 *Physica* B **210** 140
Janak J K, Moruzzi V L and Williams A R 1975 *Phys. Rev.* B **12** 1257
Jepsen O and Andersen O K 1971 *Solid State Commun.* **9** 1763
Kanomata T 1995 private communication
Kanomata T, Kikuchi M, Yamauchi Y and Kaneko T 1993 *Japan. J. Appl. Phys.* **32** 292
Lehmann G, Rennert P, Taut M and Wonn H 1970 *Phys. Status Solidi* **37** K27
Lehmann G and Taut M 1972 *Phys. Status Solidi* **54** 469
Rath J and Freeman A J 1975 *Phys. Rev.* B **11** 2109
Skriver H L 1984 *The LMTO Method* (Berlin: Springer)